# $^{68}$Ga-Citrate PET/CT for Evaluating Patients with Infections of the Bone: Preliminary Results

Cristina Nanni[1], Costantino Errani[2], Luca Boriani[3], Lorenzo Fantini[1], Valentina Ambrosini[1], Stefano Boschi[1], Domenico Rubello[4], Cinzia Pettinato[1], Mario Mercuri[2], Alessandro Gasbarrini[3], and Stefano Fanti[1]

*[1]Medicina Nucleare, Azienda Ospedaliero–Universitaria di Bologna, Policlinico S. Orsola-Malpighi, Bologna, Italy; [2]V Divisione, Istituti Ortopedici Rizzoli, Bologna, Italy; [3]Chirurgia Vertebrale, Istituti Ortopedici Rizzoli, Bologna, Italy; and [4]Medicina Nucleare, Ospedale Santa Maria della Misericordia, Rovigo, Italy*

The aim of this work was to preliminarily evaluate the sensitivity, specificity, positive predictive value, negative predictive value, and overall accuracy of $^{68}$Ga-citrate PET/CT in a population of patients with suspected bone infections. **Methods:** We enrolled 31 patients with suspected osteomyelitis or diskitis who underwent a total of forty $^{68}$Ga-citrate PET/CT scans. The results were compared with different combinations of diagnostic procedures (MRI, radiography, CT, or white blood cell scintigraphy), biopsy (when diagnostic), and follow-up data (at least 1 y) to determine the performance of $^{68}$Ga-citrate PET/CT. **Results:** We found a sensitivity of 100%, a specificity of 76%, a positive predictive value of 85%, a negative predictive value of 100%, and an overall accuracy of 90%. **Conclusion:** Although preliminary, these data confirm a possible role for $^{68}$Ga-citrate in the diagnosis of bone infections, especially in consideration of its favorable characteristics.

**Key Words:** $^{68}$Ga-citrate; PET/CT; bone infections

**J Nucl Med 2010; 51:1932–1936**
DOI: 10.2967/jnumed.110.080184

Gallium is a metallic ion that is taken up by infectious and inflammatory sites (*1*). However, $^{67}$Ga-citrate scintigraphy shows some disadvantages. The limited injectable activity (due to the long half-life) and the wide spectrum of gammas emitted by $^{67}$Ga reduce image quality and resolution. The images are low-resolution, sometimes completed by a SPECT acquisition. $^{67}$Ga is an expensive isotope and must be purchased commercially. Finally, the entire diagnostic procedure is long, lasting 3 d.

A germanium/gallium generator producing $^{68}$Ga has recently become commercially available (*2*). $^{68}$Ga is a positron-emitting gallium isotope that can be used for PET diagnostics.

Received Jun. 14, 2010; revision accepted Aug. 30, 2010.
For correspondence or reprints contact: Cristina Nanni, UO Nuclear Medicine, Azienda Ospedaliero-Universitaria di Bologna Policlinico S. Orsola-Malpighi, Via Massarenti n.9, 40138 Bologna, Italy.
E-mail: cristina.nanni@aosp.bo.it


Theoretically, the use of this isotope of gallium in the form of $^{68}$Ga-citrate presents many advantages over $^{67}$Ga for the diagnosis of bone infections. Its half-life is much shorter than that of $^{67}$Ga (just 68 min), allowing patients to be given higher tracer doses and to be discharged almost free of the radioactivity. Furthermore, the uptake phase is short, as is the whole-body image acquisition, allowing a short imaging procedure. Finally, PET/CT diagnostics produce high-spatial-resolution functional tomographic images that are then fused to low-dose anatomic CT images, exactly localizing all the pathologic findings (*3*).

Given those possible advantages of $^{68}$Ga-citrate PET/CT, the aim of this work was to preliminarily evaluate the sensitivity, specificity, positive predictive value, negative predictive value, and overall accuracy of $^{68}$Ga-citrate PET/CT in a population of patients with suspected bone infections.

## MATERIALS AND METHODS

### Patient Population

This study was approved by the Ethical Committee of our hospital. We enrolled 31 patients from January 2008 to February 2009 (18 men and 13 women; mean age ± SD, 42 ± 18 y). The patients had entered the protocol to be evaluated for acute osteomyelitis (18 patients), chronic osteomyelitis (4 patients), or diskitis (9 patients). All patients who were referred for a $^{68}$Ga-citrate PET/CT scan were suspected of having a bone infection on the basis of clinical symptoms, risk factors, inflammatory serum marker levels, and the results of standard imaging (MRI in patients without bone implants, with or without radiography). Biopsy was performed after $^{68}$Ga-citrate PET/CT.

Among the 31 patients, 7 had a bone implant or prosthesis. Twenty patients underwent $^{68}$Ga-citrate PET/CT only before therapy, 9 patients underwent two $^{68}$Ga-citrate PET/CT scans (one before therapy and the other after antibiotic therapy with or without surgical curettage), and 2 patients underwent $^{68}$Ga-citrate PET/CT only after antibiotic therapy. A total of forty $^{68}$Ga-citrate PET/CT scans were obtained (Table 1).

### $^{68}$Ga-Citrate Synthesis

$^{68}$Ga-citrate was synthesized according to the method described in a previous publication (*4*). Briefly, a $^{68}$Ge/$^{68}$Ga generator was produced by Eckert & Ziegler Isotope Products GmbH, and $^{68}$Ga-citrate syntheses were performed on a commercial adapted module used for the routine labeling of $^{68}$Ga-DOTANOC (*3*).

**TABLE 1**
Patient Population, Indication for $^{68}$Ga-Citrate PET/CT, and Final Diagnosis

| Patient no. | Sex | Age (y) | Indication for PET/CT | Timing of PET/CT* | SUVmax | | SUVmean of normal surrounding bone marrow | | Final diagnosis |
|---|---|---|---|---|---|---|---|---|---|
| | | | | | Before therapy | After therapy | Before therapy | After therapy | |
| 1 | F | 64 | Acute osteomyelitis of ankle | After therapy | | 1.4† | | 1.4‡ | TN |
| 2 | F | 63 | acute osteomyelitis of elbow | Before and after therapy | 4.8 | 3.1 | 1.1 | 1.3‡ | TP, FP |
| 3 | M | 18 | Acute osteomyelitis of tibia | Before therapy | 4.3 | | 2 | | TP |
| 4 | M | 34 | Acute osteomyelitis of tibia | Before therapy | 2.6 | | 0.8 | | TP |
| 5 | F | 32 | Acute osteomyelitis of tibia | Before therapy | 5.5 | | 0.9 | | TP |
| 6 | M | 29 | Acute osteomyelitis of tibia | Before therapy | 4.4 | | 1‡ | | TP |
| 7 | M | 58 | Acute osteomyelitis of tibia | Before therapy | 2.4 | | 1.7 | | FP (lymphoma) |
| 8 | M | 44 | Acute osteomyelitis of tibia | Before and after therapy | 3.3 | 1.5† | 2 | 1.5 | TP, TN |
| 9 | F | 60 | Acute osteomyelitis of tibia | Before therapy | 2.6 | | 0.9 | | TP |
| 10 | M | 20 | Acute osteomyelitis of tibia | Before therapy | 4 | | 1.3 | | TP |
| 11 | M | 18 | Acute osteomyelitis of tibia | Before and after therapy | 3.5 | 1.8† | 2.4 | 1.8 | TP, TN |
| 12 | M | 54 | Acute osteomyelitis of acetabulum | Before therapy | 6 | | 0.9 | | TP |
| 13 | M | 19 | Acute osteomyelitis of hip | Before therapy | 8 | | 0.8 | | TP |
| 14 | F | 20 | Acute osteomyelitis of hip | Before therapy | 7.3 | | 2 | | FP (osteoblastoma) |
| 15 | M | 51 | Acute osteomyelitis of humerus | Before and after therapy | 4.1 | 5.6 | 1.7 | 2.1‡ | TP, TP |
| 16 | M | 22 | Acute osteomyelitis of humerus | Before and after therapy | 2.5 | 1.4† | 1.2 | 1.4 | TP, TN |
| 17 | M | 51 | Acute osteomyelitis of knee (proximal tibia) | Before and after therapy | 3.1 | 1.6† | 0.8 | 1.6‡ | TP, TN |
| 18 | M | 24 | Acute osteomyelitis of tibia | Before and after therapy | 2 | 1.3† | 1 | 1.3 | TP, TN |
| 19 | M | 65 | Chronic osteomyelitis of pelvis | Before therapy | 7 | | 2 | | FP (lymphoma) |
| 20 | F | 68 | Chronic osteomyelitis of pelvis | Before therapy | 1† | | 1‡ | | TN |
| 21 | F | 47 | Chronic osteomyelitis of femur | After therapy | | 1.9† | | 1.9‡ | TN |
| 22 | M | 23 | Chronic osteomyelitis of pelvis | Before therapy | 4 | | 1.1 | | TP |
| 23 | M | 41 | Diskitis | Before and after therapy | 8.6 | 2.9† | 2.1 | 2.9 | TP, TN |
| 24 | F | 49 | Diskitis | Before therapy | 5.3 | | 2.2 | | TP |
| 25 | F | 10 | Diskitis | Before therapy | 4.1 | | 4.1 | | TN (SUVmax is high but comparable to normal bone marrow) |
| 26 | F | 71 | Diskitis | Before therapy | 2.2 | | 1.7 | | TP |
| 27 | F | 70 | Diskitis | Before therapy | 1.2† | | 1.2 | | TN |
| 28 | M | 53 | Diskitis | Before therapy | 6 | | 1.5 | | TP |
| 29 | F | 33 | Diskitis | Before and after therapy | 3.7 | 1.9† | 2.3 | 1.9 | TP, TN |
| 30 | M | 52 | Diskitis | Before therapy | 2† | | 2 | | TN |
| 31 | F | 50 | Diskitis | Before therapy | 5.6 | | 1.8 | | TP |
| Mean | | 42 | | | 4.6 | | 1.5¶ | | |

*Mean: 9 before and after therapy, 21 before therapy only, and 1 after therapy only.
†Normal value.
‡Bone implant or prosthesis; mean = 7.
¶Patient 18 was excluded.
TN = true-negative; TP = true-positive; FP = false-positive.

### $^{68}$Ga-Citrate PET/CT

All patients underwent $^{68}$Ga-citrate PET/CT (whole-body or segmental) using a 3-dimensional scanner (Discovery STE; GE Healthcare). They were intravenously injected with a mean dose of 167 MBq of $^{68}$Ga-citrate, and the uptake time was 60 min.

Fasting was not required. PET images were acquired in 3-dimensional mode for 4 min per bed position and reconstructed using a fully 3-dimensional iterative algorithm (ViewPoint algorithm [GE Healthcare], 2 iterations and 20 subsets), and attenuation correction was based on low-dose CT.

The PET/CT images were reviewed by 2 experienced nuclear medicine physicians aware of the clinical data, and the diagnosis was reached by consensus. For each patient, data about the clinical situation were accessible at the moment of the $^{68}$Ga-citrate PET/CT scan, such as the site of the pain, the presence of a bone prosthesis or implant at the site of the pain, the inflammatory marker levels, and the results of other imaging procedures. The complete imaging flow chart is reported in Supplemental Table 1 (supplemental materials are available online only at http://jnm.snmjournals.org). The scan interpretation was visual. All areas presenting tracer uptake visibly higher than the background level at the site of the suspected bone infection were considered positive. Maximum standardized uptake value (SUVmax) (normalized to body weight) was calculated lesion by lesion, and mean standardized uptake value (SUVmean) was calculated for normal bone marrow.

### Results Validation

The data were validated by comparing the PET/CT results with the results of biopsy, serum inflammatory markers (for the assessment of response to therapy), white blood cell scintigraphy, clinical follow-up, and conventional diagnostic imaging (MRI or CT in patients without a prosthesis or bone implant, or radiography). Clinical follow-up consisted of clinical evaluation of the patients approximately every 6 mo for at least 1 y.

A standard flow chart for all patients was not possible because of differences in the natural history of diskitis, acute osteomyelitis, and chronic osteomyelitis; the generally low accuracy of conventional imaging and biopsy; the inapplicability of MRI to patients with a bone implant or prosthesis; the pronounced artifacts on CT images related to bone implants; and the different therapy approaches. The final diagnosis was reached by agreement of different combinations of diagnostic procedures.

### Data Analysis

Sensitivity, specificity, positive predictive value, negative predictive value, and accuracy were calculated by comparing the PET results to biopsy (if diagnostic) or to the combination of follow-up data and conventional imaging results.

## RESULTS

### Normal Biodistribution of $^{68}$Ga-Citrate

The normal distribution is represented in Figure 1. Of interest is the relatively high vascular activity, which is not typical of $^{67}$Ga-citrate scintigraphy. $^{68}$Ga-citrate showed moderate hepatic uptake associated with mild bone marrow activity. The uptake was like that seen with $^{67}$Ga-citrate but less intense. No bowel activity was present.

### Performance of $^{68}$Ga-Citrate PET/CT

All acquired images were diagnostic.

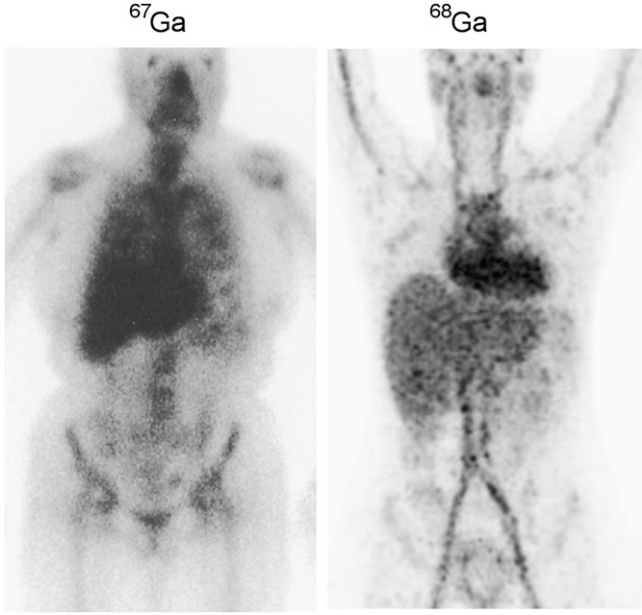


**FIGURE 1.** Physiologic biodistribution of $^{67}$Ga-citrate whole-body scintigraphy and $^{68}$Ga-citrate PET/CT.

The validation procedures are reported in Supplemental Table 1. All patients underwent biopsy, but only 11 of 30 biopsy samples (37%) were diagnostic. Details on the true-positive, true-negative, false-positive, and false-negative scans are reported in Table 1 and Figures 2–4.

Overall, we found 4 false-positive scans, 23 true-positive scans, 13 true-negative scans, and no false-negative scans, resulting in a sensitivity of 100%, a specificity of 76%, a positive predictive value of 85%, a negative predictive value of 100%, and an overall accuracy of 90%.

We did not find significant tracer uptake in uninfected bone implants.

### SUVmax Analysis

Positive $^{68}$Ga PET/CT scans presented a mean SUVmax of 4.4 ± 1.8. The SUVmax was 3.9 ± 1.8 (range, 1.7–8.0) for acute osteomyelitis, 5.5 ± 2.0 (range, 4.0–7.0) for chronic osteomyelitis, and 5.8 ± 2.0 (range, 3.7–8.6) for diskitis. Because of the small number of positive PET/CT scans performed for chronic osteomyelitis and diskitis (2 and 4, respectively), it was not possible to apply any statistical study, but the 3 groups of patients seemed to be equal because of the SUVmax overlap.

The normal bone marrow SUVmean ranged from 0.8 to 2.9. On average, the bone marrow SUVmean was 1.5. We found an increased diffuse uptake in the bone marrow of a pediatric patient (10 y old, 4.1), but this finding may represent a normal distribution in children.

## DISCUSSION

The diagnosis of bone infection has long been an issue and has been approached with several imaging methods, but

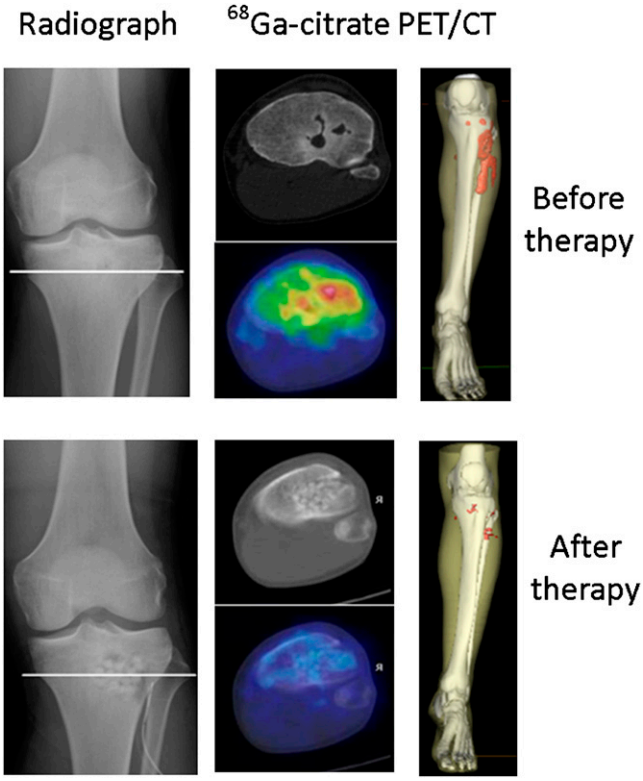


**FIGURE 2.** Comparison of $^{68}$Ga-citrate PET/CT before and after surgical curettage in patient affected by acute osteomyelitis. On right, 3-dimensional reconstruction shows bone infection (red area) also involving surrounding soft tissue. After therapy, no uptake is evident, confirming complete response.

the optimal diagnostic procedure or a standard diagnostic flow chart has not yet been identified (*5*).

Biopsy of the infected area is an invasive procedure and not always diagnostic (50% sensitivity has been reported) (*6–8*). MRI is a sensitive but nonspecific technique and is contraindicated in patients with a prosthesis or bone implant (*9*). Morphologic imaging procedures are not specific and may present significant artifacts in patients with a prosthesis. Furthermore, these tests are not reliable for the diagnosis of response to antibiotic therapy (*10,11*). WBC scintigraphy is generally sensitive and specific for the nonaxial skeleton, but the procedure is long and complicated (*12*).

Overall, bone scanning, white blood cell scintigraphy, and MRI have a sensitivity and specificity of 82%–25%, 84%–80% (21%–60% for axial skeleton), and 84%–60%, respectively (*9*). According to our results, the performance of $^{68}$Ga-citrate PET/CT is not really superior to that of a conventional imaging diagnostic flow chart (we found a slightly higher sensitivity and a comparable specificity, but the population evaluated was still limited). Its added value basically relies on a simple and fast diagnostic procedure, the absence of contraindications to scanning (no false positivity in cases of bone implants), and low dosimetry due the short half-life.

The short half-life of $^{68}$Ga-citrate, although an advantage from a dosimetric point of view, could be considered a drawback at the same time because it does not allow the long uptake time typical of $^{67}$Ga-citrate scintigraphy. This difference is illustrated by the slightly different biodistribution of the 2 compounds in the whole-body acquisition (Fig. 1). Our final results show that a short uptake time is long enough to visualize a pathologic process although a longer time would have guaranteed a higher contrast due to reduction of the background (*13*). The relatively low SUVmax, in comparison to the background, that was found in most patients with bone infection witnesses this concept. Although we used visual criteria to decide on all positive findings (and therefore the tracer uptake was significantly higher than the background), most patients had an SUVmax between 2 and 4—a value that certainly does not clearly highlight the infected area at first glance on the maximum-intensity-projection image. Each scan was therefore carefully reviewed slice by slice.

We had false-positive results in patients with tumors. This event was predictable because $^{67}$Ga-citrate has long been used as a cellularity marker. It was not possible to

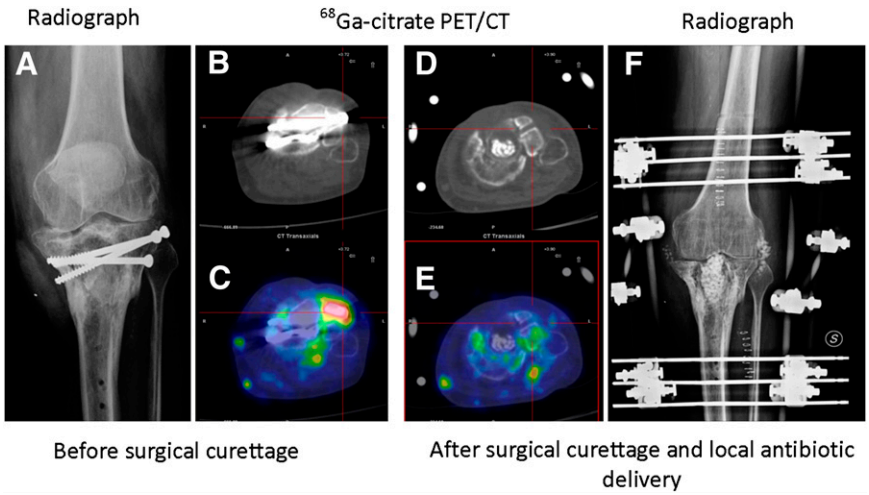


**FIGURE 3.** Comparison of $^{68}$Ga-citrate PET/CT before and after surgical curettage in patient affected by acute osteomyelitis of left tibial implant (patient 17): radiograph before therapy (A), CT scan before therapy (B), $^{68}$Ga-citrate PET/CT scan before therapy (C), CT scan after therapy (D), $^{68}$Ga-citrate PET/CT scan after therapy (E), and radiograph after therapy (F). (C) Focus of increased $^{68}$Ga-citrate uptake in lateral side of left tibial plate close to metal implant is consistent with acute osteomyelitis (SUVmax, 3.1). (E) After surgical curettage and local antibiotic delivery, tracer uptake completely normalizes. After 1 y of follow-up, patient was still free from pain.

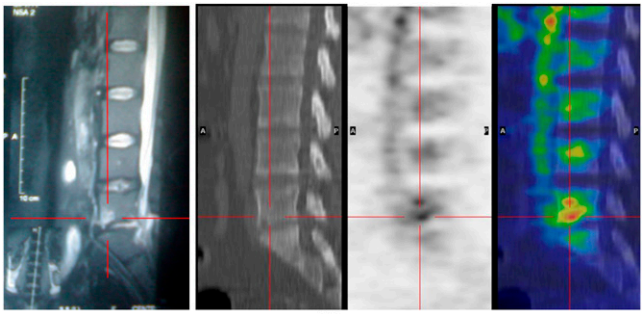


**FIGURE 4.** Comparison of spine MRI and $^{68}$Ga-citrate PET/CT in patient with diskitis. MRI shows area of abnormal signal in L5–S1 that is not unequivocally consistent with infective diskitis (patient 24). $^{68}$Ga-citrate PET/CT shows focal area of increased tracer uptake consistent with inflammation (SUVmax, 5.3).

explore causes of false positivity other than malignancies. The patient population, in fact, did not include recently operated patients or patients with recent bone fractures. Patients with bone implants showed significant artifacts on the CT images but no false-positive results in the corresponding PET series, thanks to a correction of the ViewPoint iterative algorithm.

It is interesting that no false-negative results were found and that the negative predictive value of $^{68}$Ga-citrate PET/CT was therefore quite high. This finding was confirmed by a previous preclinical publication (*14*).

The main limitation of this study concerned the gold standard used to validate the PET/CT results—a long follow-up—which is the only reliable approach due to the cited limitations of other diagnostic procedures.

The importance of functional images is not limited to the diagnosis of infection but extends also to surgical planning. The fusion of $^{68}$Ga-citrate PET images and CT images allows the surgeon to have an accurate and detailed base to better plan the operation and possibly improve patient outcome.

Many authors suggest that, besides $^{68}$Ga-citrate, the more standard $^{18}$F-FDG be used as an in vivo marker of bone infection. $^{18}$F-FDG is sensitive but has the great limitation of giving positive results in patients with a bone prosthesis, even if there is no infection or mobilization (*15*). In our population, many patients had different types of prostheses or bone implants but $^{68}$Ga-citrate was positive only in cases of infection. However, a direct comparison of the performance of the 2 tracers is important, and no more comments can be made without such a comparison.

## CONCLUSION

$^{68}$Ga-citrate PET/CT is a new diagnostic tool that can be considered in the flow chart of patients with bone infection. However, more experience is required to further validate these results.

## REFERENCES

1. El-Maghraby TA, Moustafa HM, Pauwels EK. Nuclear medicine methods for evaluation of skeletal infection among other diagnostic modalities. *Q J Nucl Med Mol Imaging.* 2006;50:167–192.
2. Ehrhardt GJ, Welch MJ. A new germanium-63/gallium-68 generator. *J Nucl Med.* 1978;19:925–929.
3. Ambrosini V, Nanni C, Zompatori M, et al. $^{68}$Ga-DOTA-NOC PET/CT in comparison with CT for the detection of bone metastasis in patients with neuroendocrine tumours. *Eur J Nucl Med Mol Imaging.* 2010;37:722–727.
4. Rizzello A, Di Pierro D, Lodi F, et al. Synthesis and quality control of $^{68}$Ga citrate for routine clinical PET. *Nucl Med Commun.* 2009;30:542–545.
5. Hughes DK. Nuclear medicine and infection detection: the relative effectiveness of imaging with $^{111}$In-oxine–, $^{99m}$Tc-HMPAO–, and $^{99m}$Tc-stannous fluoride colloid–labeled leukocytes and with $^{67}$Ga-citrate. *J Nucl Med Technol.* 2003; 31:196–201.
6. Senneville E, Morant H, Descamps D, et al. Needle puncture and transcutaneous bone biopsy cultures are inconsistent in patients with diabetes and suspected osteomyelitis of the foot. *Clin Infect Dis.* 2009;48:888–893.
7. de Lucas EM, González Mandly A, Gutiérrez A, et al. CT-guided fine-needle aspiration in vertebral osteomyelitis: true usefulness of a common practice. *Clin Rheumatol.* 2009;28:315–320.
8. Akinyoola AL, Adegbehingbe OO, Aboderin AO. Therapeutic decision in chronic osteomyelitis: sinus track culture versus intraoperative bone culture. *Arch Orthop Trauma Surg.* 2009;129:449–453.
9. Termaat MF, Raijmakers PG, Scholten HJ, et al. The accuracy of diagnostic imaging for the assessment of chronic osteomyelitis: a systematic review and meta-analysis. *J Bone Joint Surg Am.* 2005;87:2464–2471.
10. Ma LD, Frassica FJ, Bluemke DA, Fishman EK. CT and MRI evaluation of musculoskeletal infection. *Crit Rev Diagn Imaging.* 1997;38:535–568.
11. Vijayanathan S, Butt S, Gnanasegaran G, Groves AM. Advantages and limitations of imaging the musculoskeletal system by conventional radiological, radionuclide, and hybrid modalities. *Semin Nucl Med.* 2009;39:357–368.
12. Palestro CJ, Love C, Bhargava KK. Labeled leukocyte imaging: current status and future directions. *Q J Nucl Med Mol Imaging.* 2009;53:105–123.
13. Gelrud LG, Arseneau JC, Milder MS, et al. The kinetic of 67 gallium incorporation into inflammatory lesions: experimental and clinical studies. *J Lab Clin Med.* 1974;85:489–495.
14. Mäkinen TJ, Lankinen P, Pöyhönen T, Jalava J, Aro HT, Roivainen A. Comparison of $^{18}$F-FDG and $^{68}$Ga PET imaging in the assessment of experimental osteomyelitis due to *Staphylococcus aureus*. *Eur J Nucl Med Mol Imaging.* 2005;32:1259–1268.
15. Gravius S, Gebhard M, Ackermann D, Büll U, Hermanns-Sachweh B, Mumme T. Analysis of $^{18}$F-FDG uptake pattern in PET for diagnosis of aseptic loosening versus prosthesis infection after total knee arthroplasty: a prospective pilot study. *Nuklearmedizin.* 2010;49:115–123.